Effects of dilation and contraction on immersed granular column collapse

G. C. Yang, L. Jing, C. Y. Kwok and Y. D. Sobral

Abstract. Hydro-granular flow is a widespread problem characterized by the complicate fluid-particle interactions. The aim of this study is to investigate the crucial role of initial packing density in the immersed granular column collapse using the coupled lattice Boltzmann method and discrete element method. A dense case and a loose case are compared in terms of the collapsing dynamics, runout distance and induced excess pore fluid pressure. It is found that the dense case shows a dilative behavior associated with slow collapse and short runout distance with the excess pore fluid pressure being negative. While the loose case shows a contractive behavior associated with fast collapse and long runout distance with the excess pore fluid pressure being positive. These observations reveal that the macroscopic behaviors of particles collapsing in fluid heavily depends on the microscopic rheology, which is controlled by the dilation and contraction of the granular assembly.

Keywords. LBM-DEM, fluid-particle interaction, granular column collapse, dilation, contraction, packing density.

1. Introduction

Granular flows which are saturated by or immersed in fluids are ubiquitous phenomena in nature and industries, and play crucial roles in sediment transport, shaping the landscape, risk assessment and industrial optimization. In the study of debris flow via large-scale flume tests [1], it has been found that the dynamics of such hydro-granular flows heavily depends on the initial packing density. Wet sandy soil prepared in a loose state collapses rapidly on a slope. The whole assembly contracts during the failure process, resulting into partially liquefied materials. Whereas the same soil packed in a dense state only slowly creeps and dilates before a catastrophic failure.

A geometrically simplified immersed granular column collapse case has been widely applied to investigate the dynamics of granular materials in fluids both experimentally and numerically [2, 3, 4]. Rondon et al. experimentally revealed the important role of initial packing density on the dynamics of an immersed granular column collapse by measuring the induced excess pore fluid pressure at the base [2]. This laboratory study produced similar results with the debris flow flume tests [1]. The dilative and contractive regimes could also be qualitatively captured by two-dimensional (2D) numerical models, such as the distributed Lagrange multiplier/fictitious domain method [3] and the smoothed particle hydrodynamics [4].

Numerical simulations are able to offer richful information which could be hardly measured in experiments, for instance, the fluid velocity and pressure fields. However, 2D models often lead to unrealistic physical insights and limited conclusions due to the restricted kinematics. Particularly, in the case of dense granular flow with interstitial fluid, a 2D configuration will suppress the generation of turbulence and result into unreliable pore pressures due to the zero permeability caused by the discontinuous pore space, both of which can affect the granular column collapse dramatically.

The goal of this study is to investigate the effects of dilation and contraction on immersed granular column collapse via a fully-resolved three-dimensional (3D) numerical model. The lattice Boltzmann method (LBM) is applied to simulate fluids [5], while particles are simulated by the discrete element method (DEM) [6]. The fluid-particle interactions are achieved by an immersed moving boundary (IMB) technique [7].

2. Methodology

In LBM, the evolution equation with a BGK approximation (named after Bhatnagar, P. L., Gross E. P., and Krook M. [8]), can be written as:

$$f_i\left(\mathbf{x}+\mathbf{c}_i\delta_t, t+\delta_t\right) - f_i\left(\mathbf{x}, t\right) = -\frac{1}{\tau}\left[f_i\left(\mathbf{x}, t\right) - f_i^{eq}\left(\mathbf{x}, t\right)\right]. \tag{2.1}$$

where the density distribution function f_i is related to the number of molecules at time t positioned at $\mathbf{x}$ moving with velocity c_i along the ith direction at each lattice node. The time step and the relaxation time are denoted as δ_t and τ, respectively. The equilibrium distribution function f_i^{eq} is adopted as a Maxwellian one [9]. In this study, 3D LBM simulations with 19 discrete velocities (denoted as D3Q19 lattice structure [9]), which offers a good balance between accuracy and efficiency, are carried out. Based on the conservation of mass and momentum, the macroscopic fluid density ρ and velocity $\mathbf{u}$ can be easily reconstructed from the velocity moments of the density distribution functions:

$$\rho_f = \sum_{i=0}^{18} f_i, \tag{2.2}$$

$$\rho_f \mathbf{u} = \sum_{i=0}^{18} \mathbf{u}_i f_i. \tag{2.3}$$

The pressure p is related to the fluid density by the equation of state [10]:

$$p = c_s^2 \rho_f. \tag{2.4}$$

The speed of sound is c_s and equal to $1/\sqrt{3}$ in lattice units for the D3Q19 lattice arrangement [10].

While the fluid is simulated using LBM, DEM is adopted to take care of the solid particles [6]. The particle-particle collisions are governed by a simplified Hertz-Mindlin contact model [11], with the normal and tangential contact forces calculated as follows:

$$F_n = k_n \delta_n + c_n \Delta u_n, \tag{2.5}$$

$$F_t = \min\left(\left| k_t \int_{t_{c,0}}^{t_c} \Delta u_t \mathrm{d}t + c_t \Delta \mathbf{u}_t \right|, \mu F_n \right), \tag{2.6}$$

where k_n and c_n are the stiffness and damping coefficient in the normal direction. The relative normal velocity is denoted as Δu_n. k_t and c_t are the stiffness and damping coefficient in the tangential direction, the relative tangential velocity is denoted as Δu_t, and μ is the smaller of the friction coefficients of the two particles in contact. The integral represents the elastic deformation of the particle surface since contact from time $t_{c,0}$ to t_c. the magnitude of the tangential force is limited by the Coulomb friction μF_n, at which the two contacting particles start to slide against each other.

By considering the gravity ($\mathbf{G}$), contact forces and torques ($\mathbf{F}_c = \mathbf{F}_n + \mathbf{F}_t$ and $\mathbf{T}_c$) and hydrodynamic forces and torques ($\mathbf{F}_f$ and $\mathbf{T}_f$), the linear and angular velocities of particles can be calculated according to the Newton's second law:

$$m\mathbf{a} = \mathbf{F}_c + \mathbf{F}_f + \mathbf{G}, \tag{2.7}$$

$$I\dot{\boldsymbol{\omega}} = \mathbf{T}_c + \mathbf{T}_f, \tag{2.8}$$

where m and I are the mass and moment of inertia of particles, respectively. The acceleration is $\mathbf{a}$ and the angular velocity is $\boldsymbol{\omega}$. By taking the time integral of Eq. (2.7) and Eq. (2.8), the position and orientation of particles can be updated.

The coupling between LBM and DEM is achieved by the IMB method, initially proposed by Noble and Torczynski [7]. The basic principle of the IMB method is to introduce a new collision operator, right-hand side of Eq. (2.1), which depends on the solid ratio ε for a specific lattice cell. The value of ε is estimated by a cell decomposition method, and ranges between 0 (fluid cell) and 1 (solid cell). In this way, Eq. (2.1) can be rewritten as:

$$f_i\left(\mathbf{x}+\mathbf{c}_i\delta_t, t+\delta_t\right) - f_i\left(\mathbf{x}, t\right) = -\frac{1}{\tau}\left(1-B\right)\left[f_i\left(\mathbf{x}, t\right) - f_i^{eq}\left(\mathbf{x}, t\right)\right] + B\Omega_i^s, \quad (2.9)$$

where B is a weighting function of the solid ratio ε and the relaxation time τ [7]:

$$B(\varepsilon, \tau) = \frac{\varepsilon(\tau - 1/2)}{(1-\varepsilon) + (\tau - 1/2)}, \quad (2.10)$$

and Ω_i^s is the collision operator for solid cells. To ensure the no-slip boundary condition between fluid and solid, a non-equilibrium bounce-back form is adopted [12]:

$$\Omega_i^s = f_{-i}(\mathbf{x}, t) - f_{-i}^{eq}(\rho_f, \mathbf{u}_f) + f_i^{eq}(\rho_f, \mathbf{u}_s) - f_i(\mathbf{x}, t), \quad (2.11)$$

where $\mathbf{u}_f$ and $\mathbf{u}_s$ are the macroscopic fluid and solid velocities at the position of the lattice node $\mathbf{x}$. The subscript $-i$ denotes the opposite direction of i.

The hydrodynamic force $\mathbf{F}_f$ can be calculated by summing the momentum transfer along all directions at lattice cells covered by the solid particle with total number of n, which gives:

$$\mathbf{F}_f = \sum_{j=1}^{n} B_j \sum_{i=0}^{18} \Omega_i^s \mathbf{c}_i. \quad (2.12)$$

The hydrodynamic torque $\mathbf{T}_f$ is the cross product of the force and the corresponding lever arm, which can be written as:

$$\mathbf{T}_f = \sum_{j=1}^{n} \left[B_j(\mathbf{x}_j - \mathbf{x}_s) \times \sum_{i=0}^{18} \Omega_i^s \mathbf{c}_i \right], \quad (2.13)$$

where $\mathbf{x}_s$ is the center of mass of the solid particle. And $\mathbf{x}_j$ is the coordinates of the j-th lattice cell.

To synchronize the fluid and particle simulations, 100 sub-cycles of DEM calculation are conducted for every step of LBM calculation. During the sub-cycling process, the hydrodynamic force $\mathbf{F}_f$ and torque $\mathbf{T}_f$ acting on the particles remain unchanged.

3. Results and discussion

3.1. Numerical model

The coupled LBM-DEM method introduced in Section 2 was applied to simulate the collapse of a granular column in fluid, as shown in Fig. 1. A granular column was first prepared using the gravitational deposition method, which was stopped from collapsing by a vertically positioned gate. A dense and a loose packings were achieved by setting the particle friction coefficient to be 0.0 and 1.0, which were later adjusted to 0.4 before releasing the granular column. The tank with dimension

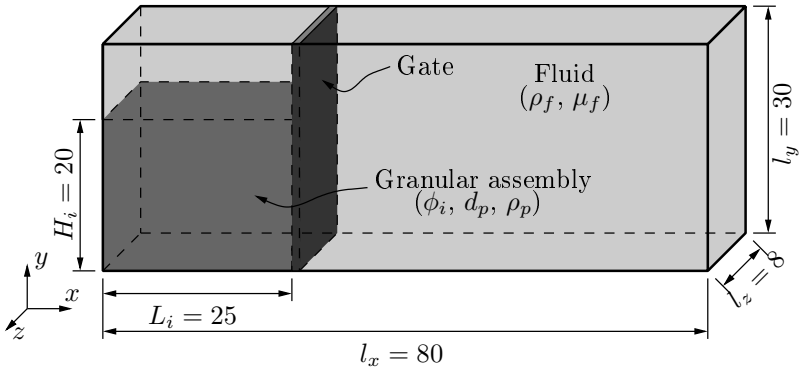

FIGURE 1. Sketch of a granular column immersed in a fluid. The granular particles are released by removing the gate (unit: mm).

TABLE 1. Modeling parameters used in the LBM-DEM simulation of immersed granular column collapse.

	Parameters	Values
Particle	Diameter, d_p	0.8 mm
	Density, ρ_p	2500 kg/m^3
	Young's modulus, E	1E9 Pa
	Poisson's ratio, ν	0.24
	Coefficient of restitution, e	0.65
Fluid	Density, ρ_f	1000 kg/m^3
	Dynamic viscosity, μ_f	0.01 Pa·s
Granular column	Initial length, L_i	25 mm
	Initial height, H_i	20 mm
	Initial packing density, ϕ_i	0.621 (dense case)
		0.565 (Loose case)

80×30×8 mm in x-, y-, and z-direction was then filled with fluid. Table 1 lists the key modeling parameters.

The granular particles were released by removing the gate, then collapsing onto the horizontal plane. Both the fluid and particle phases were constrained by solid walls in the x and y directions. While in the z direction, periodic boundaries were defined. It was found that simulations with longer periodic length produced very similar results. A resolution with 20 number of lattice cells per one particle diameter was adopted to solve the fluid-particle interactions. The whole simulation lasted for 1.904 s at which all particles almost stopped.

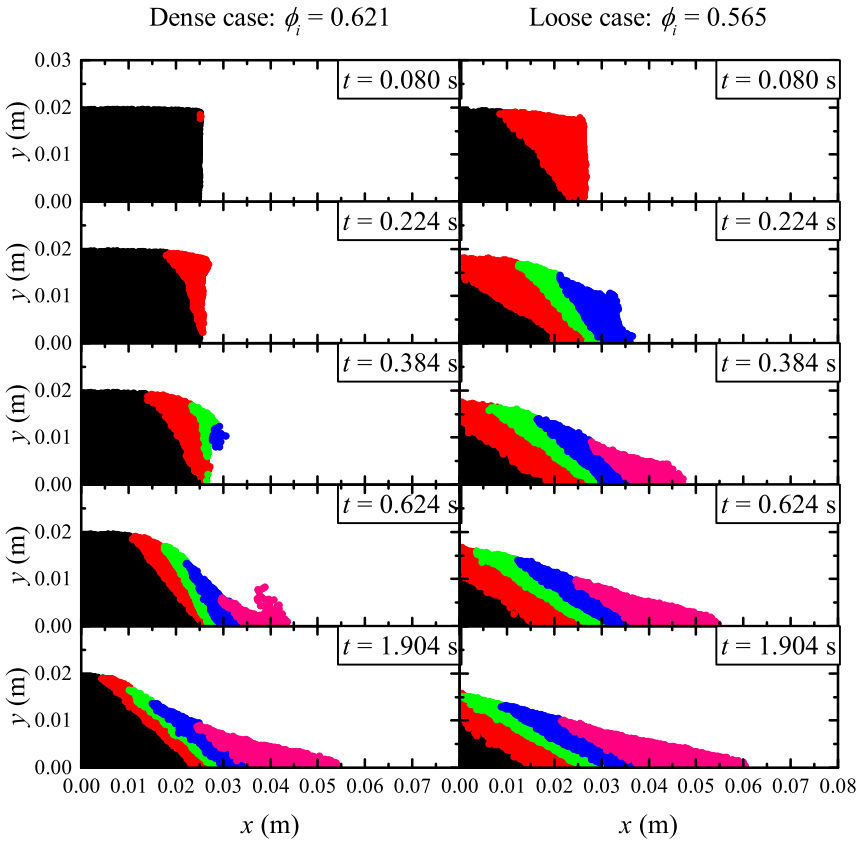

FIGURE 2. Snapshots of particles during the granular column collapse in fluid: dense case (left) and loose case (right). The particles are painted according to displacements in the xy-plane: black ($\delta_{xy} \leq d_p$); red ($d_p < \delta_{xy} \leq 5d_p$); green ($5d_p < \delta_{xy} \leq 10d_p$); blue ($10d_p < \delta_{xy} \leq 20d_p$); pink ($\delta_{xy} > 20d_p$).

3.2. Numerical results

Figure 2 shows the time sequence of collapsing particles, which are painted according to their displacements in the xy-plane (δ_{xy}). At a short time after the gate removal as $t = 0.08$ s, a large portion of particles at the top-right corner in the loose case have already started to move downwards and rightwards. At the same time in the dense case, only several particles at the top-right corner show a sign of movement and the whole granular column remains in a rectangular shape. As time goes on, the particles in the loose case continue to slide down rapidly (loose: $t = 0.224$ to 1.904 s), and at the same time spread in the horizontal direction.

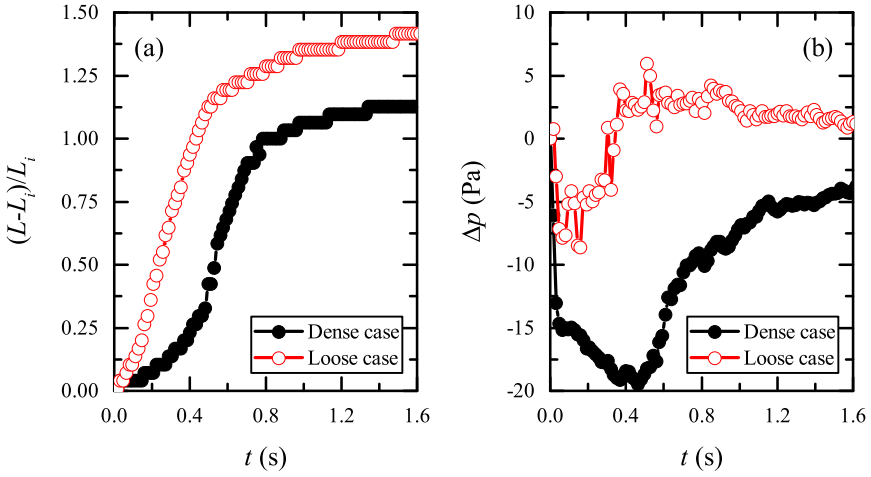

FIGURE 3. Comparison between the dense and loose cases in terms of the time evolution of runout distance and excess pore fluid pressure.

While in the dense case, the collapsing of granular column starts with a vertical fall of particles at the top-right corner (dense: $t = 0.224$ to 0.384 s). A cloud of particles at the front is formed by the induced eddies and pressurized fluid at the base (dense: $t = 0.624$ s), showing richful interactions between the fluid and the particles. At last, the particles in the dense case also spread horizontally (dense: $t = 0.624$ to 1.904 s) with continuous fall of particles at the upper slope.

The current initial aspect ratio of the granular column is small and equal to 0.8. For the loose case, nearly all particles move during the collapse, except a small portion at the left-bottom corner. The final deposition is in a triangular shape. However, for the dense case, a large number of particles close to the left-bottom corner move less than one d_p of distance in the xy-plane. The final deposition is in a trapezoidal shape.

The runout distance, normalized by the initial column length L_i, is plotted against the time in Fig. 3(a). It can be seen that the loose case collapses much faster than the dense case, which agrees with the observations in Fig. 2. The final normalized runout distance in the loose case is about 1.45, which is longer than that in the dense case with a value of 1.19.

Figure 3(b) shows the variation of the induced excess pore fluid pressure at a point (4, 3.8, 4) mm, which keeps as a fluid node during the collapse for both the dense and loose cases. The immediate collapse of particles in the loose case is caused by the induced positive excess pore fluid pressure due to the contraction of the granular column, which can push the particles away. The induced negative excess pore fluid pressure at the early state ($t < 0.4$ s) is caused by the quick

separation of particles at the top-right corner. While in the dense case, the generated negative excess pore fluid pressure due to the granular column dilation tends to hold the particles and retard the collapse. The effects of contraction and dilation remains during the whole collapsing process based on the fact that there are non-zero excess pore fluid pressures even when the particles have already stopped.

4. Concluding remarks

In this work, we have presented an efficient coupled LBM-DEM framework, which is successfully applied to solve the hydrodynamic interactions between the particles and the fluid during the granular column collapse at the pore-scale. By comparing a dense case and a loose case, it reveals two different regimes depending on the initial packing density. When the granular column has a large packing density, it collapses slowly and produces a small runout distance with the final deposition being trapezoidal. In contrast, when the initial packing density is small, the granular column collapses in a much faster rate, and gives a longer runout distance with the final deposition being triangular. The crucial role of initial packing density on the collapse of granular column in fluid can be explained by the pore pressure feedback mechanism proposed in the context of debris flows. Dilation occurs in the dense case, resulting into negative excess pore fluid pressure which can stabilize the whole granular column due to the increased effective stress. Meanwhile, contraction takes place in the loose case, resulting into positive excess pore fluid pressure which can produce partially fluidized particles.

In future works, we plan to further investigate the effects of microscopic parameters that might provide insights to the mechanism of granular flows in viscous fluids and help to develop a more reliable macroscopic continuum model.

References

[1] R.M. Iverson, M.E. Reid, N.R. Iverson, R.G. LaHusen, M. Logan, J.E. Mann, D.L. Brien, *Acute Sensitivity of Landslide Rates to Initial Soil Porosity.* Science **290** (2000), 513–516.

[2] L. Rondon, O. Pouliquen, P. Aussillous, *Granular collapse in a fluid: Role of the initial volume fraction.* Physics of Fluids **23** (2011), 073301.

[3] V. Topin, Y. Monerie, F. Perales, F. Radjaï, *Collapse Dynamics and Runout of Dense Granular Materials in a Fluid.* Physical Review Letters **109** (2012), 188001.

[4] C. Wang, Y. Wang, C. Peng, X. Meng, *Dilatancy and compaction effects on the submerged granular column collapse.* Physics of Fluids **29** (2017), 103307.

[5] S. Chen, G.D. Doolen, *Lattice Boltzmann method for fluid flows.* Annual Review of Fluid Mechanics **30** (1998), 329–364.

[6] P.A. Cundall, O.D. Strack, *A discrete numerical model for granular assemblies.* Geotechnique **29** (1979), 47–65.

[7] D.R. Noble, J.R. Torczynski, *A Lattice-Boltzmann Method for Partially Saturated Computational Cells.* International Journal of Modern Physics C **09** (1998), 1189–1201.

[8] P.L. Bhatnagar, E.P. Gross, M. Krook, *A Model for Collision Processes in Gases. I. Small Amplitude Processes in Charged and Neutral One-Component Systems.* Physical Review **94** (1954), 511–525.

[9] Y. Qian, D. d'Humières, P. Lallemand, *Lattice BGK models for Navier-Stokes equation.* Europhysics Letters **17** (1992), 479.

[10] X. He, L.-S. Luo, *Lattice Boltzmann Model for the Incompressible NavierStokes Equation.* Journal of Statistical Physics **88** (1997), 927–944.

[11] A. Di Renzo, F.P. Di Maio, *Comparison of contact-force models for the simulation of collisions in DEM-based granular flow codes.* Chemical Engineering Science **59** (2004), 525–541.

[12] Q. Zou, X. He, *On pressure and velocity boundary conditions for the lattice Boltzmann BGK model.* Physics of Fluids **9** (1997), 1591–1598.

Acknowledgment

This research is conducted in part using the research computing facilities and/or advisory services offered by Information Technology Services, the University of Hong Kong and under the support of FAP-DF, Brazil.

G. C. Yang
The University of Hong Kong
Haking Wong Building
Pokfulam Road
Hong Kong
e-mail: gengchao712@outlook.com

L. Jing
The University of Hong Kong
Haking Wong Building
Pokfulam Road
Hong Kong
e-mail: lljing@hku.hk

C. Y. Kwok
The University of Hong Kong
Haking Wong Building
Pokfulam Road
Hong Kong
e-mail: fiona.kwok@hku.hk

Y. D. Sobral
Universidade de Brasília
Campus Universitário Darcy Ribeiro
70910-900 Brasília, DF
Brazil
e-mail: yurisobral@gmail.com